A lagrangian curvilinear finite element

T. M. V. Kaiser* — A. E. Elwi**
A. Mioduchowki**

* *Centre for frontier engineering research*
200 Karl Clark Road
Edmonton, Alberta, Canada, T6N 1E2

** *Department of civil engineering*
University of Alberta
Edmonton, Alberta, Canada, T6G 2G7

ABSTRACT. *A total lagrangian formulation is developed in terms of a general orthogonal curvilinear coordinate system. The formulation is used to develop an axisymmetric finite element in cylindrical coordinates to model large displacement nonlinerarities arising out of large non-axisymmetric displacements. An axisymmetric shell under asymmetric loads and an axisymmetric beam-column are modelled to demonstrate this capability.*

RÉSUMÉ. *On établit une formulation lagrangienne totale en termes de système des coordonnées curvilinéaires orthogonales. On utilise la formulation pour établir un élément fini axisymétrique dans des coordonnées cylindriques, en vue de modéliser des grandes non-linéarités de déplacement provenant de grands déplacements non-axisymétriques. On utilise pour démontrer cette capacité le modèle d'une coque axisymétrique soumise à des pressions asymétriques et d'une traverse et d'un montant axisymétriques.*

KEY WORDS : *curvilinear, Fourier decomposition, lagrangian, large displacement, nonlinear, finite element, cylindrical, axisymmetric, non-axisymmetric, asymmetric.*
MOTS-CLÉS : *curvilinéaire, décomposition de Fourier, lagrangien, grand déplacement, non linéaire, élément fini, cylindrique, axisymétrique, non axisymétrique, asymétrique.*

Revue européenne des éléments finis. Volume 3 – n° 2/1994, pages 167 à 185

List of Symbols

X_i	Material (original) curvilinear coordinates
x_i	Spatial (deformed) curvilinear coordinates
u_i	Curvilinear displacement components
E_{ij}	Green - Lagrange strain tensor
S_{ij}	Second Piola - Kirchoff stress tensor
F_i	Specific body force components
T_i	Surface traction components
$\Delta\varepsilon_{ij}$	Infinitessimal part of Green - Lagrange strain increment
$\Delta\varepsilon'_{ij}$	First order displacement gradient (large rotation) part of Green - Lagrange strain increment
$\Delta\varepsilon''_{ij}$	Second order displacement gradient (large strain) part of Green - Lagrange strain increment
$\Delta\varepsilon'''_{ij}, \Delta\varepsilon''''_{ij}$	Higher order displacement gradient parts of Green - Lagrange strain increment
C_{ij}	Deformation tensor
C_{ijkl}	Constitutive tensor
δ_{ij}	Kronecker Delta
H^i	Material scale functions
h^i	Spatial scale functions
F_{ij}	Deformation gradient tensor
$[b]$, $[b']$	Infinitessimal and large rotation strain - displacement transformation matrices
$[d]$, $[d']$	Displacement gradient parts of $[b]$, $[b']$
$[h]$, $[h']$	Scale function parts of $[b]$, $[b']$
$[k_g]$	Geometric stiffness operator matrix
$[k^D]$	displacement gradient part of $[k_g]$
$[k^H]$	scale function part of $[k_g]$
$[k^{DH}]$	mixed part part of $[k_g]$

$[N]$ Element interpolation function matrix

$P_n(R, Z)$ Polynomial interpolation function

$\{u\}$ Element displacement vector

1. Introduction

In recent years, applications involving axisymmetric bodies subject to large non-axisymmetric deformation have assumed increasing importance. The performance demanded of Oil Country Tubular Goods (OCTG) is increasing as new recovery techniques are developed. Examples include horizontal well designs which require pipe and connections to withstand flexural loads. Large formation movements produced by subsidence or thermal recovery techniques produce high shear and bending loads on well tubulars through complex casing/formation interactions. Often, the products used in these applications were never designed with such loads in mind. Indeed, the loading mechanism itself in the casing/ formation interaction problem is one requiring a great deal of study. However, proper inelastic large deformation three dimensional analysis of these problems has been difficult to achieve because of the enormous computational effort.

A possible alternate approach is to use axisymmetric elements which utilize the initial geometric symmetry of these problems, and formulate the elements to allow for non-axisymmetric deformations. A cylindrical coordinate system in the context of a Total Lagrangian formulation seems appropriate for these elements.

Formulations for solid finite elements have been largely based on Cartesion reference systems [BAT 82], [ZIE 77], [ADI 87]. Many programs use cylindrical, spherical, or local coordinate systems for input convenience, then transform the values to global Cartesian coordinates for the finite element formulation. While significant efforts have been devoted to cylindrical formulations, most efforts have been restricted to small displacements [WIL 65], [WIN 79] or shell elements [SPI 81], [KLE 83], [CHA 70], [CHA 76], [CHA 77], [WUN 89].

This paper discusses a basic Lagrangian finite element formulation in general orthogonal curvilinear coordinate systems. It includes the basic elements for describing Lagrangian strains and strain increments in orthogonal curvilinear coordinate systems, and the procedure for integrating these into the virtual work equation, which forms the basis of most structural finite element applications. This generalized formulation is applied to a solid cylindrical finite element which is demonstrated at the end of the paper. Although developed to address structural problems in the oil industry, the formulation developed herein is general with much broader application potential.

2. Lagrangian Strains In Curvilinear Coordinates

Lagrangian formulations are able to model nonlinear behaviour arising out of large displacements, rotations, and strains. The Green-Lagrange strains on which

these formulations are based have the desirable characteristic of remaining invariant under rigid body rotation. In this section, the Green Lagrange strains, strain increments and strain increment variations are developed in terms of general orthogonal curvilinear coordinate systems.

2.1 Deformation Gradient Strain

Many authors express Green-Lagrange strains in terms of the deformation gradient in general curvilinear or orthogonal curvilinear coordinate systems [BAT 82], [MAL 69], [FUN 65], [TRU 60]. The development which follows is based largely on Malvern's discussion[MAL 69].

The Lagrangian strain tensor is defined to give the change in the squared length of the material vector in terms of the material (or reference) coordinates:

$$(ds)^2 - (dS)^2 = 2dS_i E_{ij} dS_j \qquad [1]$$

where dS_i is the original material vector, ds_i is the deformed or strained material vector, X_i are the material (original) coordinates, and E_{ij} is the Green-Lagrange strain tensor.

The deformed length is given using the deformation tensor, C_{ij}:

$$(ds)^2 = dS_i C_{ij} dS_j \qquad [2]$$

The Green-Lagrange strain tensor is thus:

$$E_{ij} = \tfrac{1}{2}(C_{ij} - \delta_{ij}) \qquad [3]$$

The material vector components are functions of position:

$$dS_i = H^i dX_i, \quad ds_i = h^i dx_i \text{ (no sum)} \qquad [4]$$

where H^i are the material scale functions, h^i are the spatial scale functions, and x_i are spatial coordinates.

In orthogonal coordinate systems, the covariant and contravariant components are coincident, and only one component type need be considered. Therefore, the convention of summation for repeated subscript indices is introduced in [4].

The spatial components may be expressed in terms of the material components through the deformation gradient tensor, F_{km}, and used in the deformation tensor:

$$ds_k = \frac{h^k}{H^m}\left(\frac{\partial x_k}{\partial X_m}\right) dS_m = F_{km} dS_m \qquad [5]$$

$$C_{ij} = F_{ki} F_{kj} \qquad [6]$$

When this is substituted into [2] and expanded, the expression for Green-Lagrange strain becomes:

$$E_{ij} = \frac{1}{2}\left(\frac{(h^k)^2}{H^i H^j} \frac{\partial x_k}{\partial X_i} \frac{\partial x_k}{\partial X_j} - \delta_{ij} \right) \qquad [7]$$

2.2 Displacement Based Strain

In finite element applications it is necessary that the strains be expressed in terms of the displacement field. This requires that appropriate displacement measures be defined. In Cartesian formulations the scale factors are unity and are independent of location, and of displacements. With other coordinate systems, however, location dependent scale functions add some complexity, and it is at this point that most authors simplify their discussions to infinitesimal strain formulations [MAL 69], [FUN 65]. Small displacement formulations in cylindrical coordinates [WIL 65], [WIN 79] typically use physical displacements as degrees of freedom. Assuming that the displacements are infinitesimally small relative to the dimensions of the body also suggests that the scale functions are independent of displacement, and a simple relationship between physical displacements and coordinate changes can be stated:

$$u_i^p = H^i(x_i - X_i) \qquad [8]$$

The superscript p on the displacement u denotes the physical displacement measure. Appropriate substitution of physical displacements into the small strain tensor gives the expressions used in most cylindrical finite element formulations.

Defining physical displacements which include deformation dependent scale functions is more difficult, and unnecessary. Instead, coordinate displacements can be used as the field variables. This approach was used by Truesdell and Toupin [TRU 60] for Lagrangian strains in general curvilinear coordinate systems, however, it has not previously been used in incremental form for a finite element formulation. Coordinate displacements eliminate the ambiguities in the relationships between physical displacements, defined displacements and displacement increments, and enables sufficient simplification of the Green-Lagrange strains to develop a generalized incremental finite element formulation in orthogonal curvilinear coordinate systems. The displacements are defined simply as:

$$u_i^c = x_i - X_i \text{ , } (i = r, \theta, z \text{ , in a cylindrical system}) \text{ ,} \qquad [9]$$

in which the superscript c indicates the coordinate displacement measure. Since this paper focusses on a coordinate displacement based formulation, the superscript c will be dropped, and all displacements will refer to coordinate measures in the following.

Differentiating [9] with respect to material coordinates, the unscaled deformation gradient tensor is obtained as

$$\frac{\partial x_i}{\partial X_j} = \frac{\partial X_i}{\partial X_j} + \frac{\partial u_i}{\partial X_j} \quad \text{or} \quad x_{i,j} = \delta_{ij} + u_{i,j} \text{ .} \qquad [10]$$

Substituting this into [7] the Green-Lagrange strains can then be expressed strictly in terms of the displacement field and scale functions:

$$E_{ij} = \frac{1}{2}\left[\frac{1}{H^i H^j}\left(h^{j^2} u_{j,i} + h^{i^2} u_{i,j} + h^{k^2} u_{k,j} u_{k,i} + h^{k^2} \delta_{kj} \delta_{ki} \right) - \delta_{ij} \right] \qquad [11]$$

The first three terms are displacement gradient components, similar to the usual expressions developed for Cartesian systems. The last two terms are less familiar pure scale factor components. In a cylindrical coordinate system, for example, the Θ (hoop) strain arising from pure radial expansion is a scale factor component.

2.3 Strain Increments

In incremental nonlinear finite element solutions, the incremental strains are expressed in terms of the incremental displacement field. The strains, displacements, and scale functions after an increment are written in terms of the values before the increment and the incremental values:

$$^{t+\Delta t}E_{ij} = {}^{t}E_{ij} + \Delta E_{ij} \qquad [12a]$$

$$^{t+\Delta t}u_i = {}^{t}u_i + \Delta u_i \qquad [12b]$$

$$^{t+\Delta t}h^i = {}^{t}h^i + \Delta h^i \qquad [12c]$$

where $'E_{ij}$, $'u_i$ and $'h^i$ are the strains, displacements and scale functions at time t, and the left superscript $t+\Delta\ t$ denotes a quantity after the increment.

Substituting each of these into the Green-Lagrange strains after the increment, expanding and subtracting $'E_{ij}$, the strain increment tensor, ΔE_{ij}, is recovered. For convenience, this is split into parts corresponding to the order of displacement increment:

$$\Delta E_{ij} = \Delta\varepsilon_{ij} + \Delta\varepsilon'_{ij} + \Delta\varepsilon''_{ij} + \Delta\varepsilon'''_{ij} + \Delta\varepsilon''''_{ij} , \qquad [13]$$

in which

$$2H^i H^j \Delta\varepsilon_{ij} = (h^{i\ 2}\Delta u_{j,i} + h^{j\ 2}\Delta u_{i,j}) + (2h^k \Delta h^k \delta_{ki}\delta_{kj}) , \qquad [14a]$$

$$2H^i H^j \Delta\varepsilon'_{ij} = \left(\begin{array}{c} h^{k\ 2}(u_{k,j}\Delta u_{k,i} + \Delta u_{k,j} u_{k,i}) \\ +2(h^j \Delta h^j u_{j,i} + h^i \Delta h^i u_{i,j} + h^k \Delta h^k u_{k,j} u_{k,i}) \end{array} \right), \qquad [14b]$$

$$2H^iH^j\Delta\varepsilon''_{ij} = \left\{ \begin{array}{c} h^k\,{}^2\Delta u_{k,j}\Delta u_{k,i} \\ +\Delta h^j\,{}^2u_{j,i} + \Delta h^i\,{}^2u_{i,j} + \Delta h^k\,{}^2(u_{k,j}u_{k,i} + \delta_{kj}\delta_{ki}) \\ +2\left[\begin{array}{c} h^j\Delta h^j\Delta u_{j,i} + h^i\Delta h^i\Delta u_{i,j} \\ +h^k\Delta h^k(u_{k,j}\Delta u_{k,i} + u_{k,i}\Delta u_{k,j}) \end{array} \right] \end{array} \right\}. \qquad [14c]$$

Note that $\Delta\varepsilon$ is a first order strain component which does not depend on the displacement gradient, and corresponds to the infinitesimal strain. The second term, $\Delta\varepsilon'$, is also a first order strain increment component, but is nonlinear because it depends on the displacement gradients at time t. The remainder of the terms are second, third and fourth order strain increment components. The first and second order terms are used in the finite element stiffness matrix formulation which follows. Higher order terms are not shown, as they are ignored in the linearization of the equations. While the stiffness matrix is therefore not exact, the error introduced by this assumption is eliminated by equilibrium iterations.

3. The Principle Of Incremental Virtual Work

The formulation for nonlinear structural finite element programs is based on the principle of virtual work. Although integrated over the deformed volume and surface of the body, the equation may be expressed in terms of the original configuration, and expressed in incremental form [BAT 82] as:

$$\int_{V_o} \delta(\Delta\varepsilon_{ij} + \Delta\varepsilon'_{ij})C_{ijkl}(\Delta\varepsilon_{kl} + \Delta\varepsilon'_{kl})dV_o + \int_{V_o} S_{ij}\delta\Delta\varepsilon''_{ij}dV_o = \qquad [15]$$

$$\int_{\Gamma}(T_i + \Delta T_i)\delta\Delta u_i d\Gamma + \int_{V_o} \rho_o(F_i + \Delta F_i)\delta\Delta u_i dV_o - \int_{V_o} S_{ij}\delta(\Delta\varepsilon_{ij} + \Delta\varepsilon'_{ij})dV_o$$

where ρ_0 is the undeformed mass density, T_i and F_i are the surface traction components and specific body force components, S_{ij} is the Second Piola-Kirchhoff stress tensor, and C_{ijkl} is the material constitutive tensor. The quantities T_i, F_i, S_{ij} and C_{ijkl} are defined at the start of the increment. Here it is assumed that the incremental stress tensor, ΔS_{ij} ,is a linear function of the first order strain increment only ($\Delta\varepsilon + \Delta\varepsilon'$).

4. Finite Element Equations

4.1 Linear Stiffness Matrix

The first term in [15] represents what will be the incremental linear stiffness matrix in the finite element form. The first order strain increments can be expressed in terms of the displacement increments in matrix form:

$$\{\Delta\varepsilon\} = [b]\{\Delta u\}, \quad \{\Delta\varepsilon'\} = [b']\{\Delta u\}, \qquad [16]$$

where $[b]$ is the linear differential operator matrix ,$[b']$ is the differential operator matrix for large rotations, $\{\Delta\varepsilon\}$ is the vector of infinitesimal strain components, $\{\Delta\varepsilon'\}$ is the vector of large rotation strain components, and $\{\Delta u\}$ is a vector of displacement field component functions.

The differential operator matrices $[b]$ and $[b']$ each have a set of components based on the displacement gradient field increment which are simply scaled versions of those of Bathe[BAT 82]. These are the first terms in each of [14a] and [14b]. The last terms, however, are scale function increments which produce components not usually seen because they vanish in Cartesian formulations. The differential operator matrices can be stated symbolically to show these components separately:

$$[b] = [d] + [h], \quad [b'] = [d'] + [h'] \qquad [17]$$

where $[d]$ contains the small displacement gradient component of $[b]$, $[h]$ contains the corresponding scale function component, and $[d']$ and $[h']$ contain the equivalent large rotation components of $[b']$.

Using [17], the first term on the left hand side of [15] can be written as:

$$\int_{V_o} \{\delta\Delta u\}^{\mathrm{T}}[b + b']^{\mathrm{T}}[C][b + b']\{\Delta u\}dV_o \qquad [18]$$

Details of the components of $[b]$ and [b']are given in Appendix I.

4.2 Geometric Stiffness Matrix

The second term on the left hand side of [15] represents the second order virtual work and leads to the geometric or nonlinear stiffness matrix. The second order component of the strain increment, [14c], can be decomposed further into subsets in the same manner that $\Delta\varepsilon$ and $\Delta\varepsilon'$ were decomposed in the previous discussion. However, because second order terms are involved, three subsets can be defined: second order displacement gradient components, second order scale function components, and cross terms including products of first order displacement gradient and first order scale function components.

A similar approach to that used to obtain [18] is adopted here so that those components similar to conventional polynomial based formulations can be illustrated distinctly. The usual approach is to express the second term on the left side of [15] in matrix form in terms of the displacement field:

$$\int_{V_o} S_{ij}\delta\Delta\varepsilon''_{ij}dV_o = \int_{V_o} \{\delta\Delta u\}^{\mathrm{T}}[k_g]\{\Delta u\}dV_o \qquad [19]$$

In the general curvilinear formulation it is easier to separate $[k_g]$ into components corresponding to the three types of components in the second order strain increment variation:

$$[k_g] = [k^D] + [k^H] + [k^{DH}] \qquad [20]$$

where $[k^D]$ is the second order displacement gradient component, which uses a scaled version of the interpolation matrix used in conventional formulations, $[k^H]$ represents the second order scale function component, and $[k^{DH}]$ includes cross terms of first order displacement gradient and scale function components.

Details of the second order virtual work components are given in Appendix I.

4.3 Finite Element Form Of Incremental Virtual Work

The virtual work equation is integrated on an element by element basis and summed to give the total virtual work on the body. The displacement field within an element is interpolated using displacement degrees of freedom at nodal locations on the body:

$$\{u\} = [N]\{u\}^N, \qquad [21]$$

where $[N]$ is a matrix of interpolation functions, and $\{u\}^N$ is a vector of nodal displacement components.

Substituting [18] to [21] into [15], and noting that the variation in the nodal displacement increments is arbitrary, the final system of incremental finite element equations is recovered as

$$\sum_{\text{Els}} \left(\int_{V_o} [B + B']^T [C][B + B'] dV_o + \int_{V_o} [N]^T [k_g][N] dV_o \right) \{\Delta u\}^N \qquad [22]$$
$$= \sum_{\text{Els}} \left(\int_{\Gamma} [N]^T \{T_i + \Delta T_i\}^N d\Gamma + \int_{V_O} [N]^T \{F_i + \Delta F_i\}^N \rho_o dV_o - \int_{V_o} [B + B']\{S\} dV_o \right) ,$$

in which the differential operator matrix and the interpolation function matrix are combined for efficiency such that

$$[B + B'] = [b + b'][N] . \qquad [23]$$

The first term inside the summation on the left hand side of [22] represents the linear stiffness matrix, while the second term represents the geometric stiffness matrix. The first two terms on the right hand side represent the imposed loads, and the last term the internal equilibrating forces.

5. Application: Cylindrical Formulation For A Quadrilateral Axisymmetric Element And Non-Axisymmetric Deformation

The finite element formulation for general orthogonal curvilinear coordinate systems described above was implemented for a cylindrical coordinate system, with coordinates r, z, and θ. The resulting element is axisymmetric in shape, quadrilateral in the axisymmetric plane and circular in cross-section (Figure 1). Integration of the element volume is the same as for conventional axisymmetric elements.

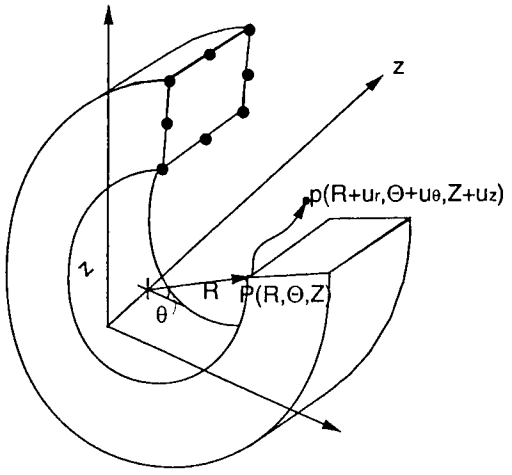

Figure 1. *Axisymmetric element for nonaxisymmetric deformation with coordinate based cylindrical displacement components*

The element displacement field is similar to that implemented by Zienkiewicz [ZIE 77], using a truncated Fourier decomposition in the circumferential direction and polynomial interpolation for the harmonic amplitute in the axisymmetric plane:

$$u_i = \sum_{n=1}^{N_p} P_n(R,Z) \sum_{f=0}^{N_f} u_{ic}^{nf} \cos(n\theta) + u_{is}^{nf} \sin(n\theta) \qquad [24]$$

where $P_n(R,Z)$ are the usual polynomial interpolation functions, N_p is the number of nodes, N_f is the number of harmonics, and $u_{i(c|s)}^{nf}$ are nodal harmonic displacement component amplitudes, with n representing the node number, f representing the fourier number, while c or s denote cosine or sine terms.

It is important to note that the displacement field is not identical to Zienkiewicz's, because the circumferential displacements are defined differently. Moreover, because the element differential operator matrix, $[B]$, contains higher order harmonic components, i.e. $\sin(\theta)\cos(\theta)$, $\sin(\theta)\sin(\theta)$, and $\sin(\theta)\cos(\theta)$ terms, and because the constitutive matrix may be nonlinear, the harmonic stiffnesses are not decoupled as they are in the linear case. Furthermore, integration of the stiffness matrix in the circumferential direction must be performed numerically. A trapezoidal rule is employed for this purpose. Thus, the computational requirements increase much more quickly as the number of harmonics is increased. However, in most cases the CPU and storage requirements are still considerabley less than those for a model based on three dimensional elements.

6. Sample Problems

The Fourier based displacement field in the circumferential direction has been well proven in linear analyses [WIL 65] and it can also be shown that the linear form of the Total Lagrangian formulation produces an identical formulation to those well established techniques. Our interest is to demonstrate the capability for modelling geometric nonlinearities. A program for Static Lagrangian Analysis of Tubular Structures (SLATS) was written to test the formulation. Two problems are presented to demonstrate the formulation. The first is an asymmetrically loaded spherical cap which has been considered by other authors [CHA 70], [CHA 76], [CHA 77]. While the element discussed here is a solid based element, it performs well when the element aspect ratio is quite high. Secondly, a cylindrical tube was modelled as an elastic beam column, with large axial and small bending loads applied. Analytical linearized buckling solutions are available for this problem [POP 78]. For comparison purposes, the same model was also analyzed using the conventional three dimensional element in ADINA [ADI 87].

6.1 Asymmetrically Loaded Cap

An axisymmetric cap under an asymmetric load is discussed by Chan and Firmin [CHA 70] and Chan and Trbojevic [CHA 76], [CHA 77] in the development of shell elements based on Fourier decomposition. Their models and results give a good basis for comparison, because the loads and results are given in terms of Fourier amplitudes, rather than the usual discrete values given by most analysts. These formulations all include kinematic assumptions which limit their effectiveness for modelling geometric nonlinearities to relatively small displacements; in the order of the shell thickness. Details of the cap and boundary conditions are given with Figure 2. The loading function given in the figure is the same as that used in [CHA 70], [CHA 76] and [CHA 77] to give a crude approximation of pressure loading over one half of the spherical cap. The pressure magnitude is equal to the analytical collapse pressure for a spherical shell, which is modified by a scale function which is increased incrementally to collapse.

A model of the same cap was prepared using SLATS. Chan's shell elements used a relatively high polynomial order in the axisymmetric interpolation of the harmonic amplitudes. Since the element discussed here was implemented with, at maximum, a quadratic order polynomial displacement field, more elements were used to analyze the cap - 20 elements versus only one in Chan's analyses, although Chan and Firmin comment that models with up to five elements exhibited the same behaviour. Harmonics up to and including 3Θ were used in both Chan's and the present analyses.

Figure 2 compares total displacement results from the solid formulation with those from Chan and Firmin [CHA 70] at two locations on the shell: at the shell apex and at the point of maximum displacement (Point B). The shell solution is initially slightly softer at both locations, but the collapse load given by both solutions is nearly identical.

Chan and Trbojevic [CHA 77] indicated that an error in the Chan and Firmin's formulation caused the finite element equations to be less stiff than they should have

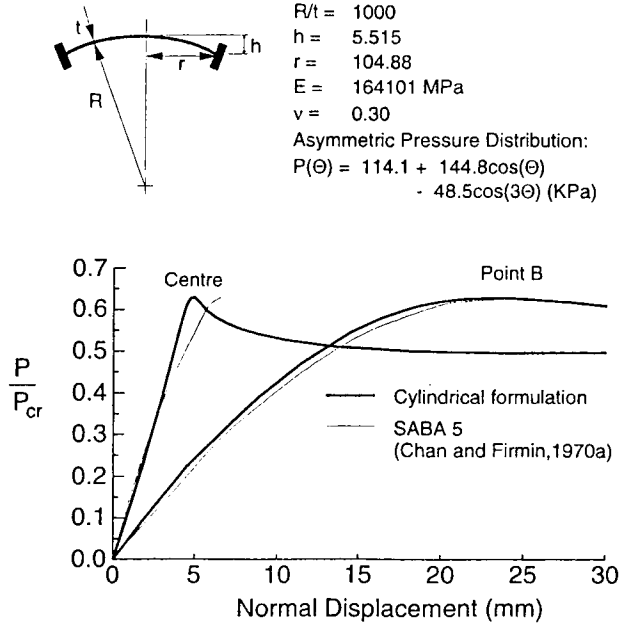

Figure 2. *Cylindrical shell under asymmetric pressure load*

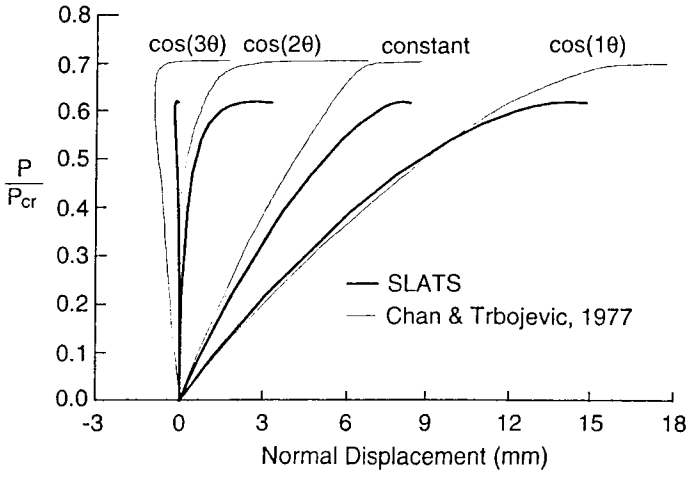

Figure 3. *Harmonic shell displacements at location of maximum deflection*

been and produced collapse loads which were artificially low. Figure 3 compares the harmonic displacement amplitudes at the maximum displacement location for the solid formulation with the shell mixed formulation of Chan and Trbojevic. While the initial stiffnesses compare better with this formulation, the collapse load given by this shell formulation is significantly higher. It is suspected that the stress distribution modelled through the shell thickness for this formulation and the coarse axisymmetric mesh employed by Chan and Trbojevic contribute to this higher stiffness. Comparing results from [CHA 70] and [CHA 77] with the present solution, it would appear that the integration error in [CHA 70] compensated for the additional stiffness due to displacement field and kinematic assumptions in those two works.

Figure 3 also illustrates the coupling between harmonics for nonlinear problems. Although there is no loading component in the 2Θ harmonic, there is a significant 2Θ component in the displacement field. As the displacements increase, the nonlinear terms become large, and the coupled displacement becomes particularly pronounced as the buckling load is approached.

6.2 Beam - Column Buckling Analysis

Figure 4 shows displacement results for a tube - column modelled with a slightly eccentric axial load. The displacements remain relatively small until the Euler buckling load is approached, at which point the displacements increase drastically at the centre. Results from the cylindrical formulation are compared with the analytical solution in Figure 4. Several transverse displacements vs. axial load curves produced using the cylindrical formulation are plotted, each showing results for a different number of harmonics. The results show excellent agreement with the analytical solution below the collapse load. However, as the collapse load is approached and the displacement becomes large, the number of harmonics must be increased for the solution to converge to the analytical solution.

The results from the highest order cylindrical formulation analysis are also compared with ADINA's conventional three dimensional formulation in Figure 5. Only the analysis with the largest number of harmonics is compared against the three dimensional model with an equivalent mesh density. The conventional formulation differs from the analytical solution at lower loads, but follows the analytical solution into the large displacement realm. The difference between the analytical and ADINA results is due to the small displacement assumptions of the linearized buckling solution and the approximation of the tube geometry and displacements by eight brick elements around the half circumference. The cylindrical formulation more accurately models the nonlinear response while the displacements are relatively small - even with few harmonics. The harmonic model stiffens artificially as translation of the beam becomes large, and the accuracy of the result deteriorates.

This implementation used the same element displacement field employed by similar elements with physical displacement field variables. Modifications are required to this displacement field description to account for the change in displacement field basis to coordinate displacements. These improvements would eliminate the lateral displacement stiffening demonstrated here and fix a problem in the global bending behaviour of the element which develops when the element diameter to

thickness ratio is small. A more complete discussion of the lateral displacement locking problem can be found in [KAI 91]

In the displacement range prior to lateral displacement locking, the results demonstrate the ability of a cylindrical based Lagrangian formulation to accurately model geometrically nonlinear behaviour.

The numerical tests demonstrate the cylindrical formulation to be more efficient in terms of execution time relative to conventional brick type solid elements. Figure 6 shows the relative times required to execute one solution step for the conventional and cylindrical formulation. The conventional formulation requires many more degrees of freedom, thus, most of the time is spent in equation solving. The cylindrical formulation, on the other hand, spends the most time generating the system of equations. Thus, as the number of elements in the axisymmetric plane increases, the solution time for the conventional model will increase much more quickly than that for the cylindrical formulation. Clearly, if the interpolation functions can be refined to model transverse rigid body motion, the cylindrical formulation can be from one to two orders of magnitude more effective for modelling the three dimensional response of axisymmetric structures.

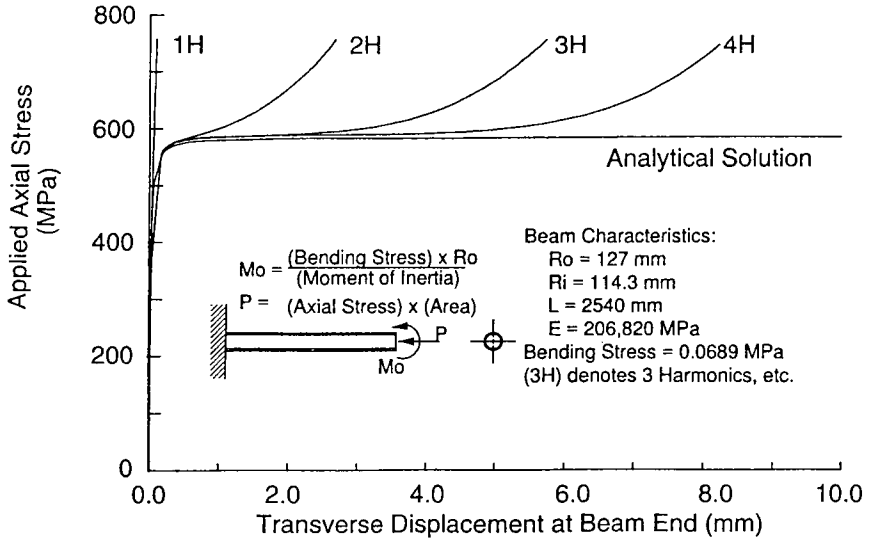

Figure 4. *Tube - column analysis results*

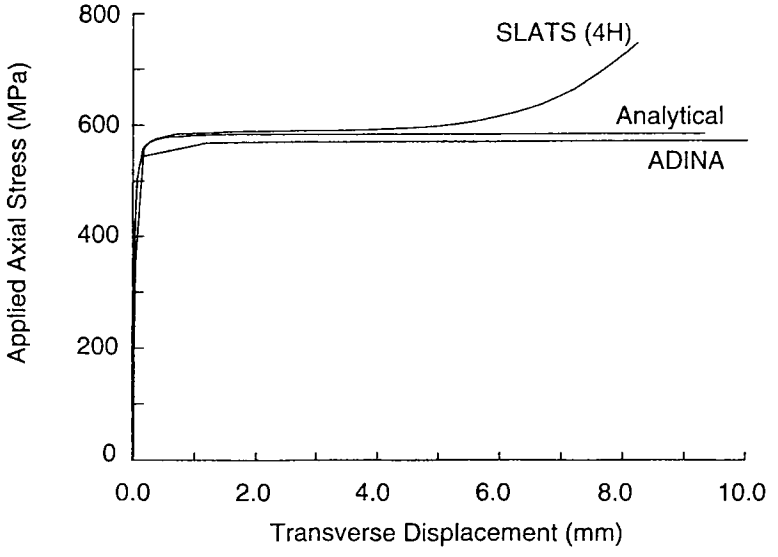

Figure 5. *Comparison of beam - column displacement results*

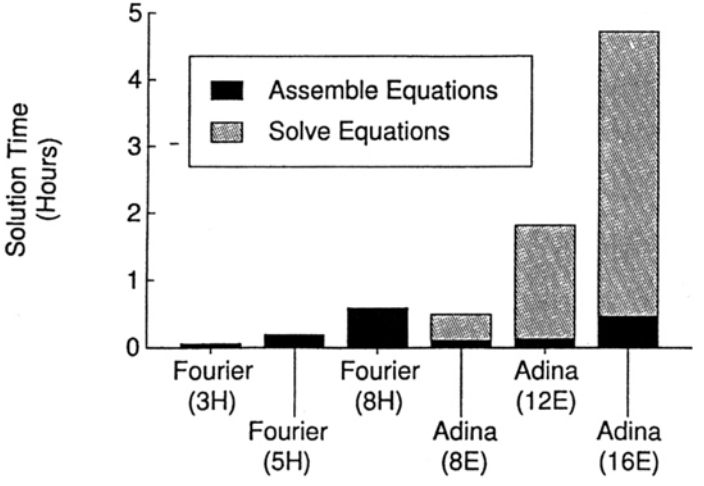

Figure 6. *Solution time comparison*

7. Conclusions

A new formulation for the finite element technique has been developed in terms of general orthogonal curvilinear coordinate systems. The formulation has been proven by application to a cylindrical element using cylindrical displacement components. The cylindrical element exactly models the geometry of axisymmetric structures, permits specification of clean boundary conditions, and accurately models nonlinear, nonaxisymmtric deformation. The element formulation demonstrated gives good solutions where rigid body translation normal to the cylindrical axis is not significant, because the element displacement field used cannot exactly model transverse rigid body displacments. It must be emphasized that the basic formulation is not at fault but it is the simple implementation of the element displacement field which causes modelling problems. Transverse motion can be approximated with reasonable accuracy by increasing the number of Fourier terms that are modelled, but translation in the order of the element radius is not possible. The deficiencies in the element displacement field have been identified for continued work to correct the element for the lateral displacement stiffening problem.

Acknowledgement

The authors wish thank the Centre for Frontier Engineering Research in Edmonton, Aberta, Canada for its support of this research project.

References

[BAT 82] Bathe, K.J., *Finite Element Procedures in Engineering Analysis*, Prentice-Hall (1982)

[ZIE 77] Zienkiewicz, O.C., *The Finite Element Method*, 3rd Ed., McGraw-Hill, New York and London (1977).

[ADI 87] *ADINA, A Finite Element Program for Automatic Dynamic Incremental Nonlinear Analysis*, Report ARD 87-1, ADINA R & D Inc, Waterton, MA. 1987

[WIL 65] Wilson, E.L., "Structural Analysis of Axisymmetric Solids," *AIAA Journal*, 1965, **12**, 2269-2274.

[WIN 79] Winnicki, L.A., and Zienkiewicz, O,C., "Plastic (or Visco-Plastic) Behaviour of Axisymmetric Bodies Subjected to Non-symmetric Loading - Semi-analytical Finite Element Solution," *Int. J. Num. Meth. Eng.*, 1979, **14**, 1399-1412.

[SPI 81] Spilker, R.L., and Daugirda, D.M., "Analysis of Axisymmetric Structures under Arbitrary Loading using the Hybrid-Stress Model", *Int. J. Num. Meth. Eng.*, 1981, **17**, 801-828

[KLE 83] Kleiber, M., and Hien, T.D., "Nonlinear Dynamics of Complex Axisymmetric Structures under Arbitrary Loads", *Comp. Meth. in Applied Mech. and Eng.*, 1983, **37**, 93-107

[CHA 70] Chan, A.S.L. and Firmin, A., "The Analysis of Cooling Towers by Matrix Finite Element Method - Large Displacements", Aeron. J. Roy. Aeron. Soc., 1970, **74**, pp. 971-982.

[CHA 76] Chan, A.S.L. and Trbojevic, V.M., "Thin Shell Finite Element by the Mixed Method Formulation", Comp. Meth. in App. Mech. and Eng., 1976, **9**, pp. 337-367.

[CHA 77] Chan, A.S.L. and Trbojevic, V.M., "Thin Shell Finite Element by the Mixed Method Formulation - Parts 2 and 3", Comp. Meth. in App. Mech. and Eng., 1977, **10**, pp. 75-103.

[WUN 89] Wunderlich, W., *et. al.*, "Semi-analytical Approach to the Nonlinear Analysis of Shells of Revolution.", Anal. Comput. Model Shell, 1989, Winter Annual Meeting ASME, pp. 509-536.

[MAL 69] Malvern, L.E., *Introduction to the Mechanics of a Continuous Medium*, Prentice-Hall, 1969.

[FUN 65] Fung, Y.C., *Foundations of Solid Mechanics*, Prentice-Hall, 1965

[TRU 60] Truesdell, C., and Toupin, R.A., "The Classical Field Theories", *Encyclopedia of Physics, Principles of Classical Mechanics and Field Theory*, Vol. III/1, Springer-Verlag New York Inc., New York, 1960

[POP 78] Popov, E.P., *Mechanics of Materials, SI Version*, Second Edition, Prentice-Hall Inc., 1978

[KAI 91] Kaiser, T.M.V., *Nonlinear Finite Element Analysis of Axisymmetric Solids with Asymmetric Deformations*, Ph.D. Doctoral Thesis, University of Alberta, Edmonton, Alberta, Canada, 1991.

Appendix I

Linear Strain - Displacement Matrices, Cylindrical Reference System

Infinitessimal Strains:

$$\{\Delta\varepsilon\} = [b]\{\Delta u\},\ \{\Delta u\}^{\mathrm{T}} = \left\langle\ \Delta u_r\ \ \Delta u_\theta\ \ \Delta u_z\ \right\rangle$$

$$\{\Delta\varepsilon\}^{\mathrm{T}} = \left\langle\ \Delta\varepsilon_r\ \ \Delta\varepsilon_\theta\ \ \Delta\varepsilon_z\ \ 2\Delta\varepsilon_{r\theta}\ \ 2\Delta\varepsilon_{\theta z}\ \ 2\Delta\varepsilon_{rz}\ \right\rangle$$

$$[b] = \begin{bmatrix} \frac{\partial}{\partial R} & 0 & 0 \\ 0 & \left(\frac{R+u_r}{R}\right)^2 \frac{\partial}{\partial\Theta} & 0 \\ 0 & 0 & \frac{\partial}{\partial Z} \\ \frac{1}{R}\frac{\partial}{\partial\Theta} & \left(\frac{R+u_r}{R}\right)^2 \frac{\partial}{\partial R} & 0 \\ 0 & \frac{(R+u_r)^2}{R}\frac{\partial}{\partial Z} & \frac{1}{R}\frac{\partial}{\partial\Theta} \\ \frac{\partial}{\partial Z} & 0 & \frac{\partial}{\partial R} \end{bmatrix} + \begin{bmatrix} 0 & 0 & 0 \\ \frac{R+u_r}{R^2} & 0 & 0 \\ 0 & 0 & 0 \\ 0 & 0 & 0 \\ 0 & 0 & 0 \\ 0 & 0 & 0 \end{bmatrix}$$

Deformation Gradient Strains:

$$\{\Delta\varepsilon'\} = [b']\{\Delta u\}$$

$$[b'] = [d'] + [h']$$

$$\{D\}^{\mathrm{T}} = \left\langle \; D_{11} \;\; D_{12} \;\; D_{13} \;\; D_{21} \;\; D_{22} \;\; D_{23} \;\; D_{31} \;\; D_{32} \;\; D_{33} \; \right\rangle$$

$$\{D\}^{\mathrm{T}} = \left\langle \; \frac{\partial u_r}{\partial R} \;\; \frac{1}{R}\frac{\partial u_r}{\partial \Theta} \;\; \frac{\partial u_r}{\partial Z} \;\; (R+u_r)\frac{\partial u_\theta}{\partial R} \;\; \frac{(R+u_r)}{R}\frac{\partial u_\theta}{\partial \Theta} \right.$$

$$\left. (R+u_r)\frac{\partial u_\theta}{\partial Z} \;\; \frac{\partial u_z}{\partial R} \;\; \frac{1}{R}\frac{\partial u_z}{\partial \Theta} \;\; \frac{\partial u_z}{\partial Z} \; \right\rangle$$

$$[d'] = \begin{bmatrix} D_{11}\frac{\partial}{\partial R} & D_{21}(R+U_R)\frac{\partial}{\partial R} & D_{31}\frac{\partial}{\partial R} \\ \frac{D_{12}}{R}\frac{\partial}{\partial \Theta} & D_{22}\frac{(R+u_r)}{R}\frac{\partial}{\partial \Theta} & \frac{D_{32}}{R}\frac{\partial}{\partial \Theta} \\ D_{13}\frac{\partial}{\partial Z} & D_{23}(R+u_r)\frac{\partial}{\partial Z} & D_{33}\frac{\partial}{\partial Z} \\ \left(D_{12}\frac{\partial}{\partial R} + \frac{D_{11}}{R}\frac{\partial}{\partial \Theta}\right) & (R+u_r)\left(D_{22}\frac{\partial}{\partial R} + \frac{D_{21}}{R}\frac{\partial}{\partial \Theta}\right) & \left(D_{32}\frac{\partial}{\partial R} + \frac{D_{31}}{R}\frac{\partial}{\partial \Theta}\right) \\ \left(\frac{D_{13}}{R}\frac{\partial}{\partial \Theta} + D_{12}\frac{\partial}{\partial Z}\right) & (R+u_r)\left(\frac{D_{23}}{R}\frac{\partial}{\partial \Theta} + D_{12}\frac{\partial}{\partial Z}\right) & \left(\frac{D_{33}}{R}\frac{\partial}{\partial \Theta} + D_{32}\frac{\partial}{\partial Z}\right) \\ \left(D_{11}\frac{\partial}{\partial Z} + D_{13}\frac{\partial}{\partial R}\right) & (R+u_r)\left(D_{21}\frac{\partial}{\partial Z} + D_{23}\frac{\partial}{\partial R}\right) & \left(D_{31}\frac{\partial}{\partial Z} + D_{33}\frac{\partial}{\partial R}\right) \end{bmatrix}$$

$$[h'] = \begin{bmatrix} \frac{(D_{21})^2}{(R+u_r)} & 0 & 0 \\ D_{22}\left(\frac{2}{R} + \frac{D_{22}}{(R+u_r)}\right) & 0 & 0 \\ \frac{(D_{23})^2}{(R+u_r)} & 0 & 0 \\ 2D_{21}\left(\frac{1}{R} + \frac{D_{22}}{(R+u_r)}\right) & 0 & 0 \\ 2D_{23}\left(\frac{1}{R} + \frac{D_{22}}{(R+u_r)}\right) & 0 & 0 \\ 2\frac{D_{21}D_{23}}{(R+u_r)} & 0 & 0 \end{bmatrix}$$

Second Order Strain Increment Virtual Work Matrices

$$S_{ij}\delta\Delta\varepsilon''_{ij} = \{\delta\Delta u\}^{\mathrm{T}}[[k^{\mathrm{D}}] + [k^{\mathrm{H}}] + [k^{\mathrm{DH}}]]\{\Delta u\}$$

$$[k^{\mathrm{D}}] = [b^{\mathrm{D}}]^{\mathrm{T}}[S][b^{\mathrm{D}}],\ [k^{\mathrm{H}}] = [b^{\mathrm{H}}]^{\mathrm{T}}[s][b^{\mathrm{H}}],$$

$$[k^{\mathrm{DH}}] = [b^{\mathrm{DH}}]^{\mathrm{T}}[s][b^{\mathrm{HD}}] + [b^{\mathrm{HD}}]^{\mathrm{T}}[s][b1^{\mathrm{DH}}]\mathrm{tDH}$$

$$[S] = \begin{bmatrix} [s] & [0] & [0] \\ [0] & [s] & [0] \\ [0] & [0] & [s] \end{bmatrix},\ [s] = \begin{bmatrix} S_{11} & S_{12} & S_{13} \\ S_{12} & S_{22} & S_{23} \\ S_{13} & S_{23} & S_{33} \end{bmatrix}$$

Displacement Gradient Part:

$$[b^{\mathrm{D}}]^{\mathrm{T}} = \begin{bmatrix} \frac{\partial}{\partial R} & \frac{1}{R}\frac{\partial}{\partial\Theta} & \frac{\partial}{\partial Z} & 0 & 0 & 0 & 0 & 0 & 0 \\ 0 & 0 & 0 & (R+u_r)\frac{\partial}{\partial R} & \frac{(R+u_r)}{R}\frac{\partial}{\partial\Theta} & (R+u_r)\frac{\partial}{\partial Z} & 0 & 0 & 0 \\ 0 & 0 & 0 & 0 & 0 & 0 & \frac{\partial}{\partial R} & \frac{1}{R}\frac{\partial}{\partial\Theta} & \frac{\partial}{\partial Z} \end{bmatrix}$$

Scale Function Part:

$$[b^{\mathrm{H}}] = \begin{bmatrix} \frac{D_{21}}{R+u_r} & 0 & 0 \\ \left(\frac{D_{22}}{R+u_r} + \frac{1}{R}\right) & 0 & 0 \\ \frac{D_{23}}{R+u_r} & 0 & 0 \end{bmatrix}$$

Mixed Parts:

$$[b^{\mathrm{DH}}] = \begin{bmatrix} 2D_{21} & 0 & 0 \\ 2\left(\frac{R+u_r}{R} + D_{22}\right) & 0 & 0 \\ 2D_{23} & 0 & 0 \end{bmatrix},\quad [b^{\mathrm{HD}}] = \begin{bmatrix} 0 & \frac{\partial}{\partial R} & 0 \\ 0 & \frac{1}{R}\frac{\partial}{\partial\Theta} & 0 \\ 0 & \frac{\partial}{\partial Z} & 0 \end{bmatrix}$$

$$D_{21} = (R+u_r)\frac{\partial u_\theta}{\partial R},\quad D_{22} = \frac{(R+u_r)}{R}\frac{\partial u_\theta}{\partial\Theta},\quad D_{23} = (R+u_r)\frac{\partial u_\theta}{\partial Z}$$